# Encoded and Enzyme-Activated Nanolithography of Gold and Magnetic Nanoparticles on Silicon

Bernhard Basnar, Jianping Xu, Di Li, and Itamar Willner*

*Institute of Chemistry and the Center of Nanoscience and Nanotechnology, The Hebrew University of Jerusalem, Jerusalem 91904, Israel*

*Received November 1, 2006. In Final Form: December 28, 2006*

A $C_{18}$ monolayer-functionalized Si surface is electrochemically patterned to yield a carboxylic acid-terminated pattern. Tyramine is covalently linked to the pattern to yield an encoded nanostructure for the enzyme tyrosinase. The biocatalytic oxidation of the tyramine residues yields catechol moieties that control the assembly of boronic acid-functionalized Au nanoparticles (NPs) or magnetic NPs. The different NPs are linked to the patterns by the formation of complexes between the boronic acid residues or $Fe^{3+}$ ions and the catechol ligands.

## Introduction

The organization of metal or semiconductor nanoparticles (NPs) on surfaces has attracted substantial research efforts directed toward the development of optical or electronic sensor systems, nanocircuitry, and devices.[1] Specifically, the generation of unidimensional assemblies of NPs has sparked significant scientific interest.[2] One widespread approach to obtain such assemblies is nanolithography. Since the introduction of the term "nanolithography",[3] numerous methods have been employed to create patterns of submicrometer size on various substrates.[4] The most prominent among these are photolithography[5] and electron beam lithography.[6] The development of atomic force microscopy (AFM) introduced a functional tool for the nanoscale patterning of surfaces. The anodic oxidation of a Si surface using a conductive cantilever is one of the first nanolithographic patterning methods.[7] Subsequent studies have demonstrated the capabilities of AFM in the nanolithographic patterning of surfaces, and dip-pen nanolithography[8] or constructive nanolithography[9] represent exciting possibilities for the fabrication of nanostructures and devices on surfaces.[10]

An extension to these methods is found in the use of enzymes. Enzymes are highly specific catalytic units that have been used in a variety of ways in nanotechnology. Some examples include the enzyme-induced generation of NPs,[11] the use of enzymes as logic gates,[12] the "cutting and pasting" of DNA,[13] and others.[14] The combination of this high substrate specificity, coupled with the spatial accuracy of the AFM, provides a powerful tool for the patterning of nanoscale structures on surfaces. Several different approaches have already been investigated. For example, the digestion of lipid bilayers by a solubilized enzyme through the mechanical deformation of the lipid layer by an AFM tip was demonstrated.[15] Similarly, the deposition of DNAase by dip-pen lithography followed by its activation with a solution containing $Mg^{2+}$ ions led to the selective etching of a self-assembled DNA monolayer.[16] The fountain-pen deposition of trypsin onto a bovine serum albumin (BSA) layer caused the spatially confined degradation of the BSA protein,[17] whereas a protease, immobilized on an AFM cantilever, was successfully employed to decompose a self-assembled protein monolayer.[18]

In contrast to the above-mentioned applications that utilized enzymes for the etching of various organic layers, enzymes have also been applied for constructive nanolithography. Alkaline phosphatase was immobilized on a cantilever and caused the localized precipitation of an insoluble reaction product.[19] In a different approach, flavoenzymes (glucose oxidase and galactose oxidase) and alkaline phosphatase, all modified with Au NPs, were deposited on silicon by dip-pen nanolithography, and the subsequent reaction with the substrate and metal ions led to the formation of gold and silver wires, respectively.[20]

One important enzyme is tyrosinase, which converts tyrosine to L-DOPA. It is considered an important biocatalyst in the neural response system and in the development of some diseases, for example, Parkinson's disease.[21] Specifically, elevated amounts of tyrosinase were observed in certain kinds of melanoma cells, and its use as a marker for these melanoma cells was discussed.[22]

* Corresponding author. Tel: +972-2-6585272. Fax: +972-2-6527715. E-mail: willnea@vms.huji.ac.il.

(1) (a) Shipway, A. N.; Katz, E.; Willner, I. *ChemPhysChem* **2000**, *1*, 18−52. (b) Katz, E.; Willner, I. *Angew. Chem., Int. Ed.* **2004**, *43*, 6042−6108. (c) Daniel, M.-C.; Astruc, D. *Chem. Rev.* **2004**, *104*, 293−346.

(2) Tang, Z.; Kotov, N. A. *Adv. Mater.* **2005**, *17*, 951−962.

(3) Broers, A. N.; Molzen, W. W.; Cuomo, J. J.; Wittels, N. D. *Appl. Phys. Lett.* **1976**, *29*, 596−598.

(4) (a) Henzie, J.; Barton, J. E.; Stender, C. L.; Odom, T. W. *Acc. Chem. Res.* **2006**, *39*, 249−257. (b) Alexe, M.; Harnagea, C.; Hesse, D. *J. Electroceram.* **2004**, *12*, 69−88. (c) Curtis, A.; Wilkinson, C. *Trends Biotechnol.* **2001**, *19*, 97−101. (d) Kohler, M.; Fritzsche, W. *Nanotechnology: An Introduction to Nanostructuring Techniques*; Wiley: New York, 2004.

(5) Harriott, L. R.; Hull, R. In *Introduction to Nanoscale Science and Technology*; Di Ventra, M., Evoy, S., Heflin, J. R., Jr., Eds.; Springer: New York, 2004; pp 7−40.

(6) Zhou, Z. In *Handbook of Microscopy for Nanotechnology*; Yao, N., Wang, Z. L., Eds.; Springer: New York, 2005; pp 287−321.

(7) Dagata, J. A.; Schneir, J.; Harary, H. H.; Evans, C. J.; Postek, M. T.; Bennett, J. *Appl. Phys. Lett.* **1990**, *56*, 2001−2003.

(8) Ginger, D. S.; Zhang, H.; Mirkin, C. A. *Angew. Chem., Int. Ed.* **2004**, *43*, 30−45.

(9) Maoz, R.; Cohen, S. R.; Sagiv, J. *Adv. Mater.* **1999**, *11*, 55−61.

(10) Wouters, D.; Schubert, U. S. *Angew. Chem., Int. Ed.* **2004**, *43*, 2480−2495.

(11) Willner, I.; Baron, R.; Willner, B. *Adv. Mater.* **2006**, *18*, 1109−1120.

(12) (a) Baron, R.; Lioubashevski, O.; Katz, E.; Niazov, T.; Willner, I. *Angew. Chem., Int. Ed.* **2006**, *45*, 1572−1576. (b) Weizmann, Y.; Elnathan, R.; Lioubashevski, O.; Willner, I. *J. Am. Chem. Soc.* **2005**, *127*, 12666−12672.

(13) Hallett, B.; Sherratt, D. J. *FEMS Microbiol. Rev.* **1997**, *21*, 157−178.

(14) (a) Kim, J.; Grate, J. W.; Wang, P. *Chem. Eng. Sci.* **2005**, *61*, 1017−1026. (b) Wu, L.-Q.; Payne, G. F. *Trends Biotech.* **2004**, *22*, 593−599.

(15) Clausen-Schaumann, H.; Grandbois, M.; Gaub, H. E. *Adv. Mater.* **1998**, *10*, 949−952.

(16) Hyun, J.; Kim, J.; Craig, S. L.; Chilkoti, A. *J. Am. Chem. Soc.* **2004**, *126*, 4770−4771.

(17) Ionescu, R. E.; Marks, R. S.; Gheber, L. A. *Nano Lett.* **2003**, *3*, 1639−1642.

(18) Takeda, S.; Nakamura, C.; Miyamoto, C.; Nakamura, N.; Kageshima, M.; Tokumoto, H.; Miyake, J. *Nano Lett.* **2003**, *3*, 1471−1474.

(19) Riemenschneider, L.; Blank, S.; Radmacher, M. *Nano Lett.* **2005**, *5*, 1643−1646.

(20) Basnar, B.; Weizmann, Y.; Cheglakov, Z.; Willner, I. *Adv. Mater.* **2006**, *18*, 713−718.

(21) Xu, Y.; Stokes, A. H.; Freeman, W. M.; Kumer, S. C.; Vogt, B. A.; Vrana, K. E. *Mol. Brain Res.* **1997**, *45*, 159−162.

10.1021/la063185h CCC: $37.00 
Published on Web 01/30/2007

A detection scheme for tyrosinase, based on the generation of L-DOPA from tyrosine and the subsequent generation of metal NPs, which were spectroscopically probed, was developed.[23] The generated L-DOPA was also used for the generation of cross-linked protein structures.[24]

In this paper, we present a new method for the constructive nanopatterning of surfaces by encoding patterns that can be activated for further reactions by a secondary enzymatic reaction. We create lines with hydroxyphenyl moieties as the surface functional group by the anodic oxidation of a $C_{18}$ monolayer on silicon and the subsequent covalent linking of tyramine to the generated carboxylic acid end-groups. By the tyrosinase-induced conversion of the hydroxyphenyl end-group to a catechol functionality, these lines are activated toward the subsequent linkage of Au NPs modified with boronic acid residues and of magnetic NPs linked through surface $Fe^{3+}$ ions to the catechol sites.

## Experimental Section

All chemicals were obtained from Sigma and used without further purification. All AFM-based lithography and AFM measurements were performed using a Picoforce AFM with Nanoscope-IV controller (DI-Veeco, Santa Barbara, CA). Scanning electron microscope (SEM) measurements were performed using a Sirion ultrahigh-resolution SEM (FEI, USA) with an EDAX spectrometer for the energy dispersive X-ray spectroscopy (EDS) analysis.

**Particle Preparation.** The magnetic particles were prepared according to a literature procedure.[25] In brief, a 25 mL mixture of $FeCl_2$ and $FeCl_3$ (molar ratio 1:2, total iron concentration 2 M) was reacted with 250 mL of 1.5 M NaOH. The particles were collected with a magnet, washed with water and with 0.1 M tetramethylammonium bromide (TMAB) and, finally, taken up in a 0.1 M solution of TMAB. Their average size was 9 nm.

The 8 nm gold NPs were prepared following the traditional citrate reduction method.[26] In brief, citrate was added to a boiling solution of 1 mM $AuCl_4^-$ in water to a final concentration of 3.5 mM, and the solution was stirred for 30 min.

The modification of the NPs with boronic acid proceeded in two steps. First, the gold NPs were reacted with 16-mercaptohexadecanoic acid (MHDA) following a literature procedure.[27] After removing the excess MHDA by centrifugation with elimination of the supernatant solution, the particles were resuspended in 10 mM HEPES buffer of pH 7.2. To this solution, *m*-aminophenyl boronic acid (APBA, 0.1 mM), 1-[3-(dimethylamino)propyl]-3-ethylcarbodiimide hydrochloride (EDC), and *N*-hydroxysuccinimide (final concentrations 2 and 5 mM, respectively) were added and stirred for 3 h. Excess chemicals were removed by centrifugation using a Centricon YM-10 filter. The particles were taken up in 1 mL of HEPES buffer, pH 7.2, to give a final concentration of approximately $10^{-9}$ M.

**Nanolithography.** The preparation of the silicon substrates was done following a literature procedure.[28] In brief, the silicon(100) substrates with *n*-type doping (Virginia Semiconductor, Inc., USA) were washed with water, acetone, and ethanol and blow-dried in a nitrogen stream. Afterward, the substrates were cleaned in a UV/ozone chamber (Ti10×10, UVOCS, Inc., USA) for 10 min. The clean silicon was immersed into a fresh 0.5 mM solution of octadecyltrichlorosilane in xylene for 2 h, followed by a 2 min sonication (DG-1, Delta Ultrasonic Cleaners, Taiwan) in clean xylene, washing with acetone and ethanol, and blow drying in a nitrogen stream.

**Scheme 1: Reaction Scheme for the Generation of the NP-Modified Nanopatterns:**

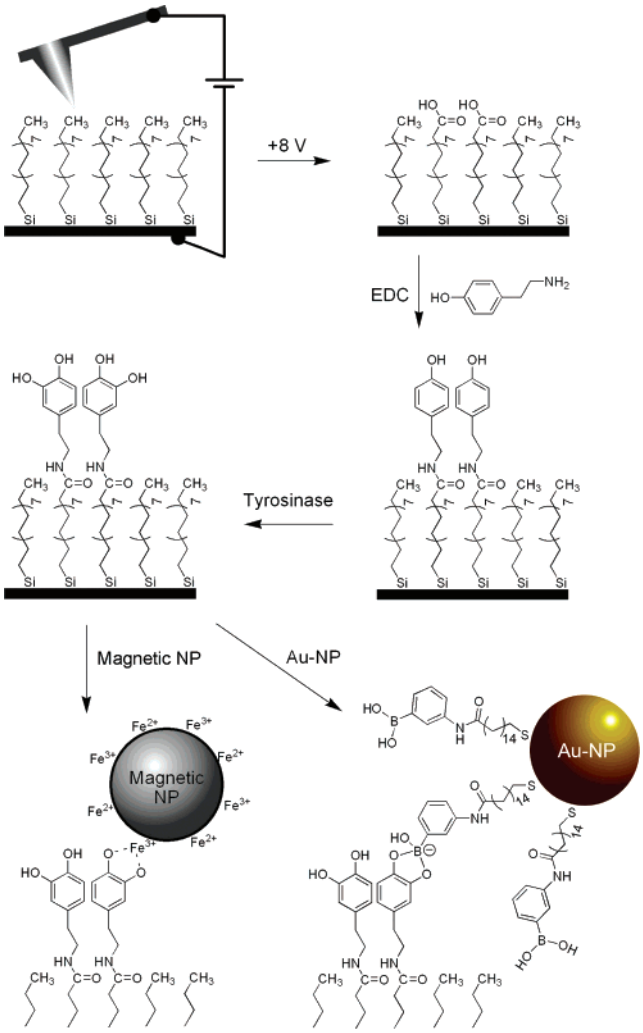


The anodic oxidation was carried out using the conducting AFM (C-AFM) mode of the AFM. For good electrical contact, the slides were glued onto metal supports using silver paint. The patterning was performed by a single pass over a 10 $\mu$m × 1 $\mu$m (for magnetic NPs) or a 10 $\mu$m × 650 nm (for gold NPs) area at a scan speed of 2 $\mu$m/s, with a measurement force of 3 nN and an applied sample bias of +8 V in an ambient environment. The cantilever in use was a contact-mode cantilever (1710-00, Topometrix) covered, by vapor deposition, with an extra layer of 50 nm of gold.

After the oxidation of the $C_{18}$ monolayer, a drop of 0.1 M tyramine (pH 6) with EDC was placed on the silicon slide and allowed to react for 30 min, followed by rinsing with water and blow drying with nitrogen. This pattern, as well as all the subsequently modified patterns, was measured in tapping mode, using NSC16 cantilevers (MikroMash, Russia).

A 10 $\mu$L drop of tyrosinase (6 U/mL) in 10 mM phosphate buffer (pH 6.5) was placed on the sample and allowed to react for 15 min, followed by rinsing with water, ethanol, and acetone, sonicating in xylene, rinsing with acetone and ethanol, and blow drying in a nitrogen stream.

The particles were attached by placing a 10 $\mu$L drop of the respective particle solution onto the slide and allowing it to react for 30 min, followed by washing with water.

## Results and Discussion

The magnetic particles (maghemite, $\gamma$-$Fe_2O_3$) were prepared according to a literature procedure,[25] and their average size was

(22) Kounalakis, N.; Goydos, J. S. *Curr. Oncol. Rep.* **2005**, *7*, 377−382.
(23) Baron, R.; Zayats, M.; Willner, I. *Anal. Chem.* **2005**, *77*, 1566−1571.
(24) Chen, T.; Embree, H. D.; Wu, L.-Q.; Payne, G. F. *Biopolymers* **2002**, *64*, 292−302.
(25) (a) Lyon, J. L.; Fleming, D. A.; Stone, M. B.; Schiffer, P.; Williams, M. E. *Nano Lett.* **2004**, *4*, 719−723. (b) Jeong, J.; Ha, T. H.; Chung, B. H. *Anal. Chim. Acta* **2006**, *569*, 203−209.
(26) Grabar, K. C.; Freeman, R. G.; Hommer, M. B.; Nathan, M. J. *Anal. Chem.* **1995**, *67*, 735−743.
(27) Aslan, K.; Pérez-Luna, V. H. *Langmuir* **2002**, *18*, 6059−6065.
(28) Basnar, B.; Friedbacher, G.; Brunner, H.; Vallant, T.; Mayer, U.; Hoffmann, H. *Appl. Surf. Sci.* **2001**, *171*, 213−225.

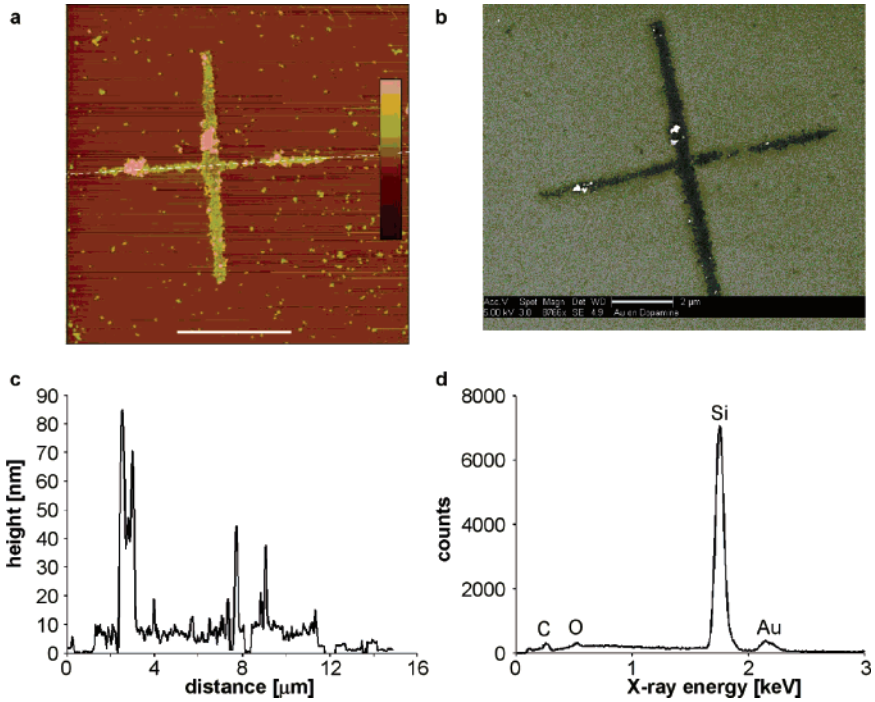


**Figure 1.** AFM and SEM characterization of Au NPs pattern: (a) AFM tapping-mode height image of the tyrosinase-treated pattern after deposition of the boronic acid-modified Au NPs. Height scale is 20 nm, and the scale bar is 5 $\mu$m. (b) SEM image of the same pattern. The scale bar is 2 $\mu$m. (c) Height profile along the dashed line in panel a. (d) EDS spectrum of the pattern.

in the range of 9 nm, in accordance with the literature.[25] The 8 nm Au NPs were prepared following the traditional citrate reduction method,[26] followed by modification with MHDA, following a literature procedure,[27] and modification with APBA. The modification of the Au particles was followed spectroscopically (see Figure S1 in the Supporting Information). The citrate-stabilized Au NPs showed a peak at $\lambda_{max} = 522$ nm. This absorbance band is broadened and shifted to $\lambda_{max} = 530$ nm and $\lambda_{max} = 537$ nm for the MHDA- and APBA-modified particles, respectively. Also, the APBA-modified particles exhibited a distinct peak at a wavelength of 268 nm, which indicates the successful linkage of the APBA to the particles.

The modification of the silicon substrates with the $C_{18}$ monolayer was performed using the reported method.[28] The assembly of the particles onto nanopatterns followed the steps depicted in Scheme 1. The first step involved the nanolithographic anodic oxidation of the $C_{18}$ monolayer to generate carboxylic acid end-groups, as was demonstrated by Sagiv et al.[9] These groups were then functionalized by tethering tyramine to the carboxylic acid residues. The tyramine residues act as suitable substrates for tyrosinase, which converted the monohydroxyphenyl moieties to catechol moieties. The resulting catechol could, in turn, bind to the magnetic NPs or the APBA-modified Au NPs.

The anodic oxidation of the methyl headgroups of the silane monolayer was carried out using the C-AFM mode of our AFM. The modification was investigated by contact-mode AFM. A strong contrast in the friction image, confirming the conversion of the surface functional group, and nearly no change in the topography were observed, indicating that the silicon substrate was not oxidized under the chosen conditions (see Figure S2 in the Supporting Information).

After the oxidation of the $C_{18}$ monolayer, the carboxylic acid moieties were modified by placing a drop of 0.1 M tyramine (pH 6) with EDC on the silicon slide and letting it react for 30 min. The AFM characterization of this pattern showed a height contrast of less than 1 nm between the lines and the surrounding substrate, as would be expected for such a small molecule (the theoretical length of tyramine is approximately 1 nm).

Then, the sample was reacted with tyrosinase by placing a drop of tyrosinase (6 U/mL) in 10 mM phosphate buffer (pH 6.5) on the sample. The AFM image did not show any changes in the height compared to the tyramine-modified layer. This is in agreement with the fact that the enzyme only introduces a second hydroxyl group and, thus, does not change the length of the molecule itself.

After this enzymatic activation of the substrate, the surfaces were reacted with the respective functionalized NPs according to Scheme 1. Figure 1a,b shows the AFM and SEM images of the resulting pattern generated upon incubation with the boronic acid-modified Au NPs. The AFM confirms that the pattern is covered with a relatively homogeneous layer of approximately 7 nm thickness with several higher features present (Figure 1c). This thickness is in good agreement with the average particle diameter. When looking at the SEM image, the same pattern is clearly visible. The EDS spectrum of the pattern (Figure 1d) shows a large silicon peak from the support and a substantially smaller, but still significant peak for gold. Control experiments reveal that no pattern of Au NPs is generated on the tyramine-functionalized monolayer that was not treated with tyrosinase (see Figure S3A in the Supporting Information). These results clearly indicate that the biocatalytic synthesis of the catechol units by tyrosinase on the encoded electrosynthesized pattern, which was functionalized with tyramine, is essential to the assembly of the boronic acid-functionalized Au NPs on the surface.

The assembly of the magnetic NPs on the catechol-functionalized pattern is shown in Figure 2. The AFM image (Figure 2a) reveals a homogeneous pattern of the NPs of about 9 nm thickness (Figure 2c), which is in good agreement with the average particle diameter. Also, some higher features of the magnetic particles are observed that, presumably, originate from the aggregation of the NPs. The SEM image shows the same pattern (Figure 2b). The elemental analysis by EDS confirms the presence of the

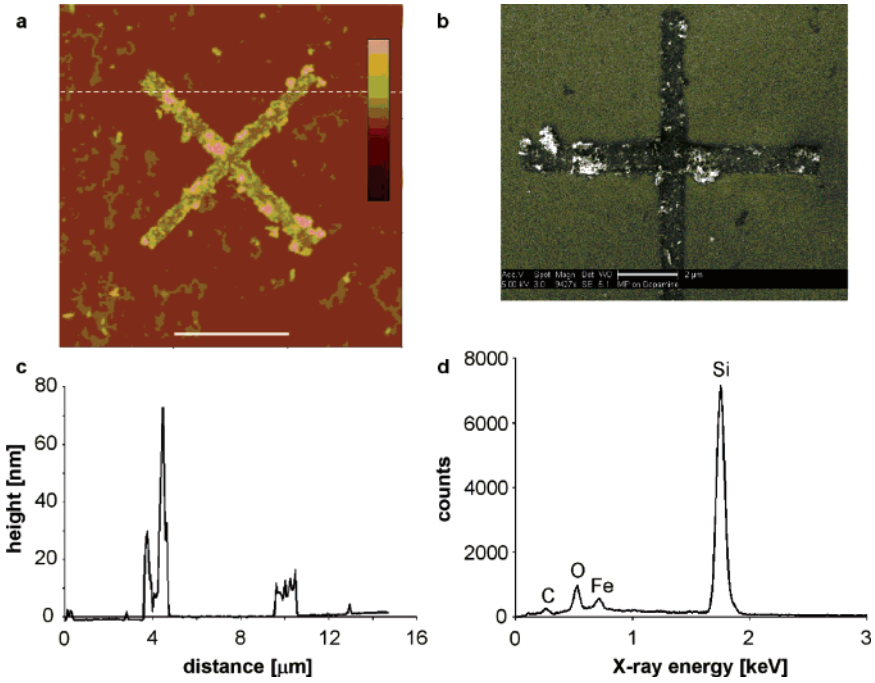


**Figure 2.** AFM and SEM characterization of magnetic NPs pattern: (a) AFM tapping-mode height image of the tyrosinase-treated pattern after deposition of magnetic NPs. Height scale is 100 nm, and the scale bar is 5 $\mu$m. (b) SEM image of the same pattern. The scale bar is 2 $\mu$m. (c) Height profile along the dashed line in panel a. (d) EDS spectrum of the pattern.

magnetic NPs, as indicated by the characteristic band of iron, with the silicon background peak dominating the spectrum (Figure 2d).

Control experiments indicated that the tyrosinase-induced synthesis of the catechol sites was essential to bind the magnetic NPs to the pattern. Treatment of the tyramine-functionalized surface with the magnetic NPs did not lead to the association of the NPs to the pattern (see Figure S3B in the Supporting Information).

As tyrosinase is known to act on catechol units used as substrates, converting them into *o*-quinones, further experiments were carried out using a 10 mM dithionite solution as a reducing agent after the enzymatic conversion, which would reduce all quinone functionalities to catechol units. The patterns, obtained after subsequent immersion into the respective particle solutions, yielded identical results (see Figure S4 in the Supporting Information), indicating that the particles are, indeed, binding to the catechol moieties.

## Conclusions

In conclusion, the present study demonstrates the feasibility of using enzymes as activating agents for the formation of nanopatterns on surfaces. By encoding the patterns with a suitable substrate (tyramine), we have been able to selectively link both Au and magnetic NPs to the pattern by the activation of the pattern with tyrosinase. This opens up new possibilities in the field of nanobiosensors, but even more so, in the field of nanocircuitry. One may envisage the formation of an encoded pattern consisting of several different substrates for various enzymes, allowing full control of the orthogonal formation of nanostructures without chemical cross-talk during the patterning.

**Acknowledgment.** This research is supported by the European Community VSN Integrated Project.

**Supporting Information Available:** UV/vis spectra of the different steps of the Au NPs preparation and modification as well as an AFM image of the control samples. This material is available free of charge via the Internet at http://pubs.acs.org

LA063185H